Density Functional Investigation of Hydrated V(II) and V(III) Ions: Influence of the Second Coordination Sphere; Water Exchange Mechanism

Meriem Benmelouka, Sabri Messaoudi, Eric Furet,* Régis Gautier, Eric Le Fur, and Jean-Yves Pivan

Département de Physicochimie, UPRES 1795, Ecole Nationale Supérieure de Chimie de Rennes, Institut de Chimie, Campus de Beaulieu, Avenue du Général Leclerc, 35700 Rennes, France

Received: August 6, 2002; In Final Form: March 11, 2003

Two aspects of the aqueous chemistry of $[V(H_2O)_6]^{2+/3+}$ have been studied at the B3LYP level of theory. The first one concerns the role of an explicit second coordination sphere of 12 water molecules on the structures of hexahydrated V(II) and V(III) ions. For the two cations, the most stable conformers correspond to a wheel-like structure in which the second hydration shell can be viewed as being constituted of three open quadrimers, each one being connected by one hydrogen bond to the other two and to three ligands of the first sphere through four additional hydrogen bonds. The $[V(H_2O)_6]^{3+}$ subunit in this conformer is found to mimic the arrangement observed in $[V(H_2O)_6][H_5O_2](CF_3SO_3)_4$ (Cotton, F. A; Fair, C. K.; Lewis, G. E.; Mott, G. N.; Ross, F. K.; Schultz, A. J.; Williams, J. M. *J. Am. Chem. Soc.* **1984**, *106*, 5319). The others conformers investigated, for which the second hydration shell consist of four noninteracting cyclic trimers, were calculated to be 15.6 kcal/mol (V^{3+}) and 13.6 kcal/mol (V^{2+}) higher in energy at the in vacuo level. These differences were increased to 22.8 kcal/mol (V^{3+}) and 18.5 kcal/mol (V^{2+}) when taking into account the bulk solvent using a polarizable continuum model. For the water-exchange mechanisms, we find that, for both cations, the D mechanism is the preferred one at the gas-phase level using density functional theory calculations. The effect of the solvent on the activation barriers ($\Delta E^{\ddagger}$) is emphasized because it induces inversions in the A−/D− and I−/D− reaction-path orderings. On the basis of the calculated $\Delta E^{\ddagger}$ values in solution, the water-exchange mechanism is expected to proceed via a limiting A pathway and an I-activation process for V^{3+} and V^{2+}, respectively. The differences between the experimental $\Delta H^{\ddagger}$ values and the computed activation barriers were found to be 0.6 kcal/mol and −2.6 kcal/mol, respectively. The effect of the hydration energy on the stability and, hence, the lifetime of the various intermediates is also discussed.

Introduction

Nowadays, the chemistry of aqua ions is still the subject of intensive theoretical and experimental research[1] because such species play important roles in many chemical and biological systems. In recent years, numerous quantum chemical studies have been devoted to one fundamental aspect of the reactivity of the hydrated metal ions, namely, the water-exchange mechanism,[2−14] especially since Rotzinger [3,4] and Hartmann et al.[5] have successfully applied an approach in which the transition states and intermediates of the various pathways were fully optimized. It was shown, indeed, that ab initio calculations of the reaction profiles using cluster models optimized in the gas phase allowed the possible mechanisms for most of the hexaaqua transition-metal ions[3−5] to be distinguished from one another. For $[V(H_2O)_6]^{3+}$, Rotzinger [4] proposed an associative mechanism and ruled out the dissociative pathway on the basis of an estimated activation barrier ($\Delta E^{\ddagger}$). For hexaaquavanadium(II), the gas-phase calculations [3] carried out at the HF level of theory led to identical $\Delta E^{\ddagger}$ values for both the interchange and dissociative reaction paths. Therefore, the exchange mechanism was attributed by comparing the activation volume ($\Delta V^{\ddagger}$) to a parameter calculated as the difference of the sums of all V−O distances between the transition state and the reactant ($\Delta\Sigma d$-(V−O)). In a later study, the water-exchange mechanism of hexaaquavanadium(II) ion was revisited by modeling the bulk solvent by a polarizable continuum medium.[9] The geometries were optimized at the HF level of theory within the Onsager solvent model.[15] The final energies were obtained by incorporating a dynamic electron correlation correction whereas the hydration energies were evaluated using a shape-adapted cavity. Adding such contributions, the activation barriers for the two water-exchange pathways became different. These results indicate therefore that solvent effects and electron correlation may significantly alter the activation energies and hence may lead to changes of the preferred water-exchange mechanism.

Because one of our current projects concerns a theoretical investigation of the condensation processes of vanadium cations under hydrothermal conditions, we report here a density functional study of two aspects of the solution chemistry of hexahydrated vanadium cations. In the first part, we will discuss the structural modifications induced on $[V(H_2O)_6]^{2+/3+}$ by the presence of an explicit second water-coordination sphere. In the next section, the water-exchange mechanisms of V(II) and V(III) will be revisited using density functional calculations and taking into account the solvent effects to cover a more dynamic aspect of the aqueous chemistry of these ions.

Methods

Model Reactions. Following the approach employed by Rotzinger et al. [3,4,6,8−12] and Hartmann et al.,[5,7] the water-

* Corresponding author. E-mail: Eric.Furet@ensc-rennes.fr.

10.1021/jp026697n CCC: $25.00
Published on Web 04/24/2003

exchange mechanisms were investigated by means of model clusters consisting of one vanadium ion surrounded by a total of seven water molecules distributed over the first and second coordination spheres. Associative (A), dissociative (D), or interchange (I) character was attributed to the various pathways on the basis of the structures of the transition states and existing intermediates. Indeed, a limiting A mechanism is characterized by a heptacoordinated intermediate whereas a limiting D mechanism presents a pentacoordinated intermediate. In both cases, the imaginary mode associated with the transition state involves the motion of one activated water molecule. Finally, reaction profiles pertaining to the I type exhibit only one symmetric transition state with the two participating molecules that are located located the same distance from the metal center. As in a previous study,[13] we also used as a qualitative mechanistic indicator for the further attribution of associatively (I_a) or dissociatively (I_d) activated character to the concerted pathways an estimated activation volume ($\Delta V^{\ddagger}$) deduced from the volume variation of the cavity in the polarizable continuum model (PCM).[16−18]

Computational Details. All of the geometry optimizations and frequency calculations were carried out with the Gaussian 98, Revision A.11.3 package[19] using the B3LYP[20,21] hybrid functional. For the basis sets, we used 6-311G(d) [22−25] for vanadium and 6-31G(d)[26,27]for oxygen and hydrogen. Such a combination of basis sets was selected after numerous unsuccessful attempts at trying to find the cis transition state (see below) for the I mechanism of V(II). We initially employed the same basis sets for all atoms starting from a guess structure of C_2 symmetry. However, it appeared that using either the 6-31G(d), 6-31++G(d,p), or 6-311G(d) basis sets and testing different functionals invariably led the calculation either to structures related to the D intermediate or failed completely to converge to any chemically relevant geometry. It seemed, therefore, that an improved description of the interaction between the metal and the activated molecules as compared to the one between those water molecules and the ligands of the first sphere was required in order to locate this transition state. Thus, we switched back to the 6-31G(d) basis sets for the water molecules and increased only the number of basis functions on the vanadium atom. It should be pointed out that once we obtained the cis transition state with our reference basis set we used this structure as an improved guess to attempt to reoptimize it with the basis sets described above on all atoms. Unfortunately, those calculations led to the same meaningless results as those previously described. A similar basis dependency has already been noted by Hartmann et al. [5] in their study of the exchange pathways of Zn(II). Using 6-311G(d) on all atoms, they were able to localize the transition states of the D mechanism with seven water molecules surrounding the metal ion whereas with larger basis sets the same structures were not obtained. They also indicated that in all cases no suitable transition state for the concerted pathway could be converged. Thus, it might be possible that by using an equivalent combination of the 6-311G(d) and 6-31G(d) basis sets such an interchange transition state could be converged. However, things may not be so simple, as from our own experience it appears that the basis set dependency is also related to the nature of the cation. Indeed, it turned out that we were able to find a cis transition state for the interchange mechanism on hydrated Cr(III) using 6-31G(d) on all atoms, but we were unsuccessful on the isoelectronic cluster $[V(H_2O)_6]^{2+}$, as previously noted.

The experimental studies of the water exchange of solvated cations gives access to thermodynamic activation parameters such as the activation enthalpy ($\Delta H^{\ddagger}$) or entropy ($\Delta S^{\ddagger}$). In the present report, we use a computed activation energy ($\Delta E^{\ddagger}$), neglecting zero-point energy and thermal corrections to distinguish between the different mechanisms and compare with experimental data. We have checked the influence of such approximations on the calculated activation barriers. It appears indeed that the differences between the computed $\Delta H^{\ddagger}$ and $\Delta E^{\ddagger}$ values are always less than 1.2 kcal/mol. Therefore, it seems reasonable to conclude, as previously discussed in a recent article[13] concerning the water-exchange mechanism in $[UO_2(H_2O)_5]^{2+}$ and $[UO_2(oxalate)_2(H_2O)]^{2-}$, that the computed activation energy gives a satisfactory approximation of the $\Delta H^{\ddagger}$ value. Neglecting the solvent effects would constitute a much cruder approximation. For this reason, we used the polarizable continuum model of Tomasi and co-workers[16−18] to evaluate the solvation energy from single-point calculations on the optimized gas-phase model clusters.

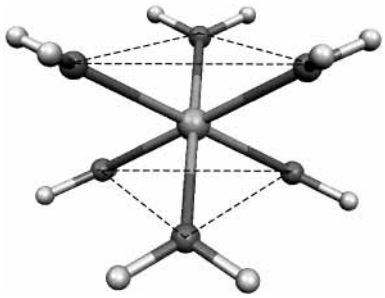

Figure 1. D_{3d} all-horizontal arrangement of the water molecules in $V(H_2O)_6$.

Results and Discussion

$[V(H_2O)_6]^{2+/3+}$ and $[V(H_2O)_6]^{2+/3+}\cdot(H_2O)_{12}$. Hexaaquavanadium d^2 and d^3 ions are found in several crystal structures. $[V(H_2O)_6]^{2+}$ occurs, for example, in $[V(H_2O)_6](CF_3SO_3)_2$,[28] in $[V(H_2O)_6]SiF_6$,[29] or in the ammonium Tutton salt $(NH_4)_2[V(H_2O)_6](SO_4)_2$.[29] The mean $V-OH_2$ distances are 2.119, 2.125, and 2.128 Å, respectively. The $[V(H_2O)_6]^{3+}$ unit has been isolated, for example, in the β-alums $M^I[V(H_2O)_6]\cdot(SO_4)_2\cdot(H_2O)_6$ [30] or in the compound $[V(H_2O)_6][H_5O_2](CF_3SO_3)_4$.[31] In those cases, the mean vanadium−oxygen distance ranges from 1.991 to 1.996 Å, and $[V(H_2O)_6]^{3+}$ could be considered to have either S_6 or D_{3d} symmetry.

For $[V(H_2O)_6]^{2+}$, we obtained in vacuo an expected structure of T_h symmetry with V−O distances equal to 2.146 Å, which is in agreement for the VO_6 core with the regular octahedron observed in the X-ray structure of $[V(H_2O)_6](CF_3SO_3)_2$.[28] Concerning the hexaaquavanadium(III) complex, an optimization under the constraints of D_{3d} symmetry using the arrangement of the water molecules found in $[V(H_2O)_6][H_5O_2](CF_3SO_3)_4$ [31] (see Figure 1) leads to a structure that was identified as a transition state. From an unconstrained optimization of $[V(H_2O)_6]^{3+}$, we obtained a minimum in which all V−O distances are equal to 2.039 Å and a geometry that deviates slightly from ideal T_h symmetry because of small angular distortions of the VO_6 octahedron as well as rotations (∼10°) of the water molecule planes about the V−O axes. Thus, the structure could be identified as having C_i symmetry. It is obvious that for such a high-spin d^2 metal-ion configuration the Jahn−Teller theorem would apply, leading to a lowering of the complex's symmetry from the highest attainable symmetry (T_h) for such a hexaaqua complex. However, much higher symmetries than C_i, such as D_{3d}, D_3, or S_6, might be expected for a high-spin $[V(H_2O)_6]^{3+}$ complex. Indeed, in the neutron diffraction and X-ray investigations of $[V(H_2O)_6][H_5O_2](CF_3-$

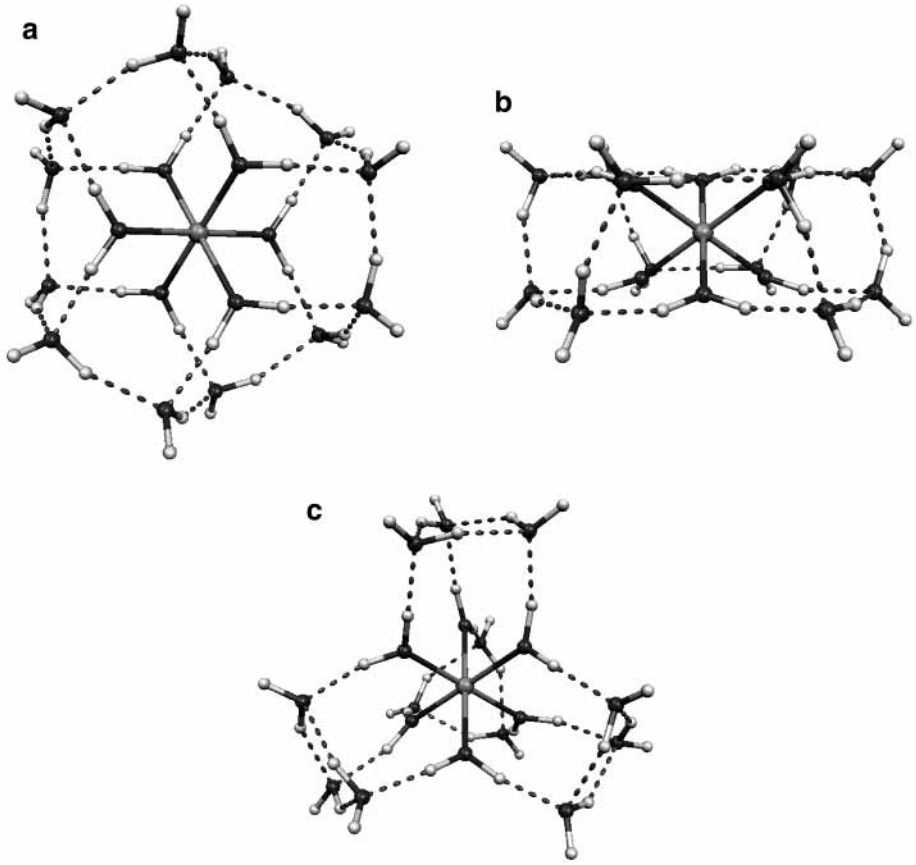

Figure 2. Structures of the two conformers of $[V(H_2O)_{18}]^{3+}$. (a) View of VIII[A] along the C_3 axis, (b) view of VIII[A] perpendicular to the C_3 axis, and (c) geometry of the D_2 model.

$SO_3)_4$, Cotton et al. [31] showed that the hexaaquavanadium(III) unit adopts a near-D_{3d} all-horizontal geometry (see Figure 1), for which a preferred e_g^2 configuration results from the splitting of the t_g orbitals when lowering the symmetry from T_h to D_{3d} all-horizontal. A rationalization of the electronic structure of $[V(H_2O)_6]^{3+}$ has been carried out by Kallies et al. [32] in order to understand these deviations in the gas phase from ideal D_{3d} symmetry. They studied the bonding interaction trends in the series of 3d hexaaqua ions using density functional theory and natural bond orbital[33] analyses. For $[V(H_2O)_6]^{3+}$, they showed that numerous stationary points, being either minima, transition states, or saddle points, can be found within an energy window of about 8 kcal/mol. One might therefore expect that strong hydrogen bonds between $[V(H_2O)_6]^{3+}$ and its environment could induce changes in the nature and the relative ordering of these structures and may lead to a different preferred arrangement of the hexaaquavanadium(III) cluster in solution. We have therefore carried out an investigation of the influence of the second coordination sphere on the geometry of this complex. The guess structure of $[V(H_2O)_6]^{3+}\cdot(H_2O)_{12}$ was build up from the previously optimized gas-phase geometry of $[V(H_2O)_6]^{3+}$ by placing 12 molecules into the second coordination sphere, each being hydrogen bonded to one water molecule of the first hydration shell. The optimization was carried out without symmetry constraints to allow for a full reorganization of the two coordination spheres. The final geometry, which can be considered to have near-S_6 symmetry, was confirmed by frequency analysis to be a true minimum on the potential energy surface. This conformer, denoted here as VIII[A], exhibits a wheel-like structure with a dense network of hydrogen bonds (see Figure 2a and b). Each water molecule of the outer hydration sphere is bonded to 1 ligand of the first sphere and 2 H_2O molecules of the second shell, resulting in a total of 24 hydrogen bonds for the conformer. The structure of the second hydration sphere can be conceptually seen to consist of three open quadrimers, each one interacting with the two others and through four hydrogen bonds with three water molecules of the first shell. It should be noted that the geometry of these quadrimers is, however, quite far from the structure of the global minimum on the potential energy surface of $(H_2O)_4$. Indeed, the water tetramer has been shown to adopt a cyclic geometry of S_4 symmetry.[34] It is immediately seen that $[V(H_2O)_6]^{3+}$ adopts a near-D_{3d} all-horizontal symmetry, as in $[V(H_2O)_6][H_5O_2](CF_3SO_3)_4$.[30] This feature is due to the particular structure of the hydrogen-bond network between the two coordination spheres that constraints the $[V(H_2O)_6]^{3+}$ subunit to deviate from its optimum gas-phase geometry. Adding the second coordination sphere leads to shorter V−O distances within the $[V(H_2O)_6]^{3+}$ core (see Table 1), which are still 0.02 Å longer than the mean experimental values found in both $M^I[V(H_2O)_6]\cdot(SO_4)_2\cdot(H_2O)_6$ [30] and $[V(H_2O)_6][H_5O_2](CF_3SO_3)_4$.[31] From this small reduction of the $V-O_I$ bonds of 0.03 Å when taking into account the second hydration shell, it might be expected that for the water-exchange mechanisms the hydration energy calculated using the gas-phase geometries would not be too different from the same quantity computed after a full optimization within the PCM method. This assumption is corroborated by a recent theoretical study of the water exchange in the hydrated UO_2^{2+} ion carried out by Vallet et al.[13] Indeed, they showed that whereas the geometry optimization of the uranyl aqua cation with CPCM led to a significant shortening (0.07 Å) of the $U-OH_2$ distances the difference in solvation energy calculated from a single-point calculation on the gas-phase structure was small.

From recent publications, we found that structures similar to

TABLE 1: Selected Geometrical Parameters for the Conformers of $[V(H_2O)_6]^{2+/3+}\cdot(H_2O)_{12}$[a]

conformer	$d(V-O_I)$	$d(H_I-O_{II})$	$d(O_{II}-H_{II})$	symmetry
VIII[A]	6x(2.012)	6x(1.700, 1.718)	6x(1.836, 1.846)	$\sim S_6$
VIII[B]	2x(1.979, 2.027, 2.052)	4x(1.687, 1.705, 1.731)	4x(1.876, 1.913, 1.932)	D_2
VII[A]	2x(2.137, 2.138, 2.140)	2x(1.828, 1.852, 1.858) 6x(1.826)	2x(1.764, 1.770, 1.777, 1.795) 4x(1.785)	$\sim C_i$
VII[B]	3x(2.137, 2.142)	3x(1.828, 1.848) 6x(1.833)	3x(1.856, 1.870) 6x(1.860)	$\sim C_3$

[a] Distances are given in Å.The I and II subscripts identify the atoms of the first and second hydration spheres, respectively.

the VIII[A] conformer have been computed for $Ti^{2+/3+}$ [35] and Mg^{2+}.[36] It was demonstrated that the wheel-like structure could be considered, at the present time, to be the global minimum on the potential energy surface of the $[M(H_2O)_6]^{n+}\cdot(H_2O)_{12}$ clusters for these ions. In their quantum chemical investigation of the coordination spheres around Mg^{2+}, Markham et al. [36] studied another minimum of *T* symmetry, previously optimized by Pye et al. [37] at the HF/6-31G* level. They found this structure to lie about 10 kcal/mol higher in energy than their new conformer of S_6 symmetry at the B3LYP/6-31G* level of theory. In the density functional study carried out by Uudsemaa et al. [35] on the cluster isoelectronic to $[V(H_2O)_6]^{3+}\cdot(H_2O)_{12}$:$[Ti(H_2O)_6]^{2+}\cdot(H_2O)_{12}$, no such structurally equivalent conformer was investigated. It should be noted that Rotzinger recently carried out an optimization at the HF level of theory of this kind of conformer when he investigated the electron self-exchange reaction via the outer-sphere pathway for $[M(H_2O)_6]^{2+/3+}$ and $[M(H_2O)_6]^{3+/4+}$ couples (M = V, Ru).[38] However, in his study, the conformer VIII[A] was not considered. We therefore optimized $[V(H_2O)_6]^{3+}\cdot(H_2O)_{12}$ under the constraints of D_2 symmetry because the Jahn−Teller theorem predicts a symmetry lowering from the *T* point group for such a high-spin d^2 metal cation. The final structure is presented in Figure 2c and will be denoted here as VIII[B]. Similar to the aforementioned $[Mg(H_2O)_6]^{2+}\cdot(H_2O)_{12}$ complex of *T* symmetry and the structure optimized by Rotzinger,[38] the second coordination sphere in the VIII[B] conformer can be viewed as being constructed from a set of four individual cyclic water trimers, each being connected by three hydrogen bonds to the first coordination sphere, resulting as for VIII[A] in a total of 24 hydrogen bonds. The arrangement of these trimers differs from the structure of the true minimum of $(H_2O)_3$ by the fact that in VIII[B] all of the nonbonded hydrogens within the trimer are located on the same side of the O_3 plane to allow for interactions between the oxygens of the trimers and the hydrogens of the first hydration shell. In VIII[B], the metal−oxygen bond distances ($V-O_I$) are different (see Table 1), as opposed to what was previously observed in our near-S_6 conformer optimized without symmetry constraints. Such differences within the VO_6 core were also reported in the structure optimized by Rotzinger. Both the $V-O_I$ (2.016, 2.048, and 2.071 Å) and H_I-O_{II} (1.710, 1.726, and 1.749 Å) distances are longer than ours, as could be expected from a treatment at HF level of theory. Concerning the gas-phase energy difference between VIII[A] and VIII[B], we found that the wheel-like conformer was more stable than the D_2 complex by 15.6 kcal/mol. Considering the gas-phase free energy gives a preference for VIII[A] over VIII[B] of 14.3 kcal/mol, indicating that the entropy contribution is almost the same for the two structures. However, taking into account the solvent effects on the gas-phase geometry using the PCM method induces an increased stabilization of VIII[A] over the D_2 complex, the difference in solvation energies being 7.2 kcal/mol. This additional energy lowering of the wheel-like structure is almost entirely due to larger electrostatic contributions to the hydration energy, which are known to be related to the cavity volume. We will see in the next section concerning the water-exchange activation processes that this parameter will play an important role because the transition states of each exchange mechanism exhibit typical shapes leading to distinctive cavity volumes and hence to different electrostatic terms for the solvation energy.

Considering an explicit second hydration shell around $[V(H_2O)_6]^{2+}$ also induces some structural perturbations of its ideal T_h gas-phase geometry. We used two structures as starting points. In the first one, the guess geometry was derived from that of VIII[A]. For the second form, we employed a conformer related to VIII[B] but having *T* symmetry. The result of the geometry optimization on this latter form led to a final conformer that the frequencies calculation showed surprisingly to be a saddle point. Lowering the symmetry to D_2 gave exactly the same conformer. Removing all of the symmetry constraints and reoptimizing the structure induced an insignificant energy stabilization of 0.05 kcal/mol. The final geometry, denoted here as VII[B], was this time a true minimum on the potential energy surface and was shown to be of near-C_3 symmetry. This result is somewhat at variance with the one computed by Rotzinger at the HF level of theory because he obtained a conformer of higher symmetry (*T*) that is structurally equivalent to VII[B]. Although it may seem problematic, this apparent discrepancy is only formal as we consider here the overall symmetry of the conformer that results from a delicate balance between several factors. On one hand, T_h symmetry is preferred for the $[V(H_2O)_6]^{2+}$ subunit, as previously described. On the other hand, optimizations without symmetry constraints, at the B3LYP/6-31G* or MP2(Full)/aug-cc-pVDZ, on one of the water trimers present in VII[B] gave us geometries that can be considered to have perfect C_3 symmetry. It should be recalled that these trimers are different from the true minimum of $(H_2O)_3$.[34] As could be expected, the computed O···H distances in the gas-phase trimer are quite different between the two theoretical models; they are in fact equal to 1.837 Å (B3LYP/6-31G*) and 1.915 Å (MP2(Full)/aug-cc-pVDZ). However, carrying out a B3LYP calculation using the aug-cc-pVDZ basis sets gives 1.913 Å. Concerning the conformer containing cyclic trimers, because we used density functional theory, we therefore have shorter (stronger) hydrogen bonds between the first and the second hydration sphere (mean value H_I-O_{II}: 1.836 Å; see Table 1) as compared to the ones computed by Rotzinger (H_I-O_{II}: 1.863 Å). Thus, we believe that in our case the overall symmetry of the conformer is dictated by the structure of the water trimers. Moreover, it seems reasonable to assume that the second hydration shell is flexible enough in these $[M(H_2O)_6]^{n+}\cdot(H_2O)_{12}$ complexes, especially in the less charged ones, so that several closely related stationary points exist that are separated only by small energy differences. However, it must be pointed out that the above results do not lead us to exclude the possibility to be able to obtain the VII[B] complex within the *T* point group using hybrid functionals and extended basis sets.

In any case, it appeared that, as for $[V(H_2O)_6]^{3+}$, VII[B] was not the most stable one. Indeed, the result of the geometry

TABLE 2: Selected Geometrical Parameters, Relative Energies in the Gas Phase and in the Solvent, Volume Changes, and Point Group Assignments for the Water Exchange Reactions of $[V(H_2O)_6]^{2+}$ [a]

species	$d(V-O_I)$	$d(V-O^{\ddagger})/d(V-O_{II})$	$\Delta E^{\ddagger}$	$\Delta E^{\ddagger}_{PCM}$	ΔV	symmetry
reactant	2.152, 2.156, 2.154, 2.134, 2.151, 2.138	−/3.906	0	0	0	C_1
I mechanism						
TS_{trans}	2.140, 2.219, 2.113	2.757/−	20.9	20.1	−0.3	C_2
TS_{cis}	2.140, 2.124, 2.122	2.858/−	17.7	17.4	+0.1	C_2
D mechanism						
TS	2.124, 2.000, 2.103, 2.110	3.371/4.242	15.0	20.6	+6.9	$\sim C_s$
intermediate	2.122, 2.102, 2.110	−/4.191	13.8	17.6	+5.5	$\sim C_{2v}$

[a] Distances are given in Å; relative energies, in kcal/mol; and volume changes, in cm^3/mol. O_I corresponds to the oxygen of a water molecule in the first sphere; $O^{\ddagger}$ refers to the oxygen of an activated ligand; and O_{II} corresponds to the oxygen of a ligand in the second sphere.

optimization on the wheel-like structure, denoted here as VII-[A], showed that this form was lying 13.6 kcal/mol, in vacuo, below the aforementioned complex and 18.5 kcal/mol in aqueous solution. VII[A] is only of near-C_i symmetry and presents three groups of identical distances (see Table 1) within the VO_6 core. It should noted that a third conformer has been localized that appeared to be in the gas phase 50.7 kcal/mol higher in energy than VII[A] and was therefore ruled out of the discussion. The second coordination sphere in this form can be described on the basis of two open and two cyclic noninteracting trimers.

Water-Exchange Processes: Structure of the Reactants. For all of the exchange pathways, we used as the reactant a structure with the water molecule in the second sphere hydrogen-bonded to two ligands of the first hydration shell. For V(III), we noted that trying to optimize an alternative structure with the seventh molecule singly hydrogen-bonded to one of the first-sphere H_2O molecules induces a spontaneous migration of a proton, which ends up in the final stable complex $[V(H_2O)_5(OH)]^{2+}\cdot H_3O^+$. Hartmann et al.[7] have already observed such a deprotonation process in their density functional investigation of the water-exchange mechanism of hexaaquatitanium(III). This feature led them to carry out calculations on the deprotonation reaction path and to investigate in more detail the dissociative pathways of $[Ti(H_2O)_5(OH)]^{2+}$. From what was obtained with the two conformers of $[V(H_2O)_6]^{3+}\cdot(H_2O)_{12}$, we can conclude, however, that the deprotonation process being activationless is an artifact that results from the limitations of the present cluster models. Indeed, whereas $[V(H_2O)_6]^{3+}$ is known to hydrolyze readily because of its low pK_a value (2.26),[39] one should obtain a chemically significant activation barrier for the deprotonation reaction when taking into account additional hydration shells. In a following paper, we will precisely comment on the results obtained concerning the successive hydrolysis reactions of hydrated vanadium cations. In any case, for V(III), we had only one possible starting-point structure at hand for the calculation of the activation barriers of the water-exchange mechanism.

For V(II), we were able to optimize both conformers using our reference basis set, which was also the case for Rotzinger [9] at the HF level of theory. However, the structure with the singly bonded H_2O molecule appeared to be, in our case, a transition state that was connected to the other conformer, the activation barrier being 2.8 kcal/mol. When using a different basis set, namely, 6-31++G(d), on all atoms, this second conformer becomes a true minimum on the potential energy surface. This feature illustrates the fact that, as previously discussed in the Computational Details section, some structures of these exchange mechanisms are quite sensitive to the choice of the basis set. However, for a distinction of the various pathways, the truly important point is the relative ordering of the transition states. The differences in energy between "several" starting-point structures were always less than 3 kcal/mol and should therefore affect only the quality of the comparison with experimental data.

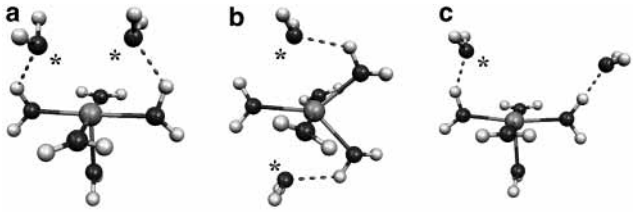

Figure 3. Optimized geometries of the transition states for the water-activation processes of $[V(H_2O)_6]^{2+}$. (a) I mechanism: activated ligands in the cis position, (b) I mechanism: activated ligands in the trans position, and (c) D mechanism. The activated water molecules are marked with a star.

Water Exchange in Hydrated V(II). From a high-pressure ^{17}O NMR experiment on $[V(H_2O)_6]^{2+}$, the activation volume ($\Delta V^{\ddagger}$) was measured to be equal to −4.1 cm^3/mol,[40] the activation enthalpy ($\Delta H^{\ddagger}$) being 14.8 kcal/mol. Because the estimated value for a limiting associative (A) mechanism was deduced to be −13.5 cm^3/mol,[41] the exchange reaction was therefore suggested to proceed through an associatively activated interchange (I_a) mechanism.

In an early theoretical study, Åkesson et al.[2] proposed a dissociative mechanism for $[V(H_2O)_6]^{2+}$. In a subsequent quantum chemical investigation, Rotzinger[3] proposed a preferred I_a mechanism on the basis of a negative $\Delta\Sigma d(V-O)$ value; the calculated $\Delta E^{\ddagger}$ quantities were almost identical for both the D and I_a pathways. Those initial calculations having been made in vacuo at the HF level of theory. In a later quantum chemical study, Rotzinger[9] confirmed this result as he succeeded in distinguishing the two reaction pathways on the basis of the activation barriers using its refined model (see Introduction). However, recent publications seem to indicate that the use of a shape-adapted cavity would be more appropriate for both the geometry and the final energy calculations.[42]

The results of our DFT investigation on hexaaquavanadium-(II) are given in Table 2. Three different transition states have been localized (see Figure 3). Two of them correspond to concerted reaction paths, and the third is of the D type because the respective imaginary modes describe the motion of two or only one water molecule. As shown in Table 2, the gas-phase calculations do not give, in our case, the same values for the interchange and dissociative mechanisms. Indeed, we obtain a preference for the D activation process over the I pathways of at least 2.7 kcal/mol. The calculated $\Delta E^{\ddagger}$ value for the D mechanism reaction is *only* 0.2 kcal/mol higher than the experimental activation enthalpy. On the basis of these results, one would therefore conclude that a D mechanism is preferred for the water-exchange process. However, it should be noted that the energy difference between the transition state and the pentacoordinated intermediate is small (1.2 kcal/mol), indicating

TABLE 3: Selected Geometrical Parameters, Relative Energies in the Gas Phase and in the Solvent, Volume Changes, and Point Group Assignments for the Water Exchange Reactions of $[V(H_2O)_6]^{3+}$ [a]

species	$d(V-O_I)$	$d(V-O^{\ddagger})/d(V-O_{II})$	$\Delta E^{\ddagger}$	$\Delta E^{\ddagger}_{PCM}$	ΔV	symmetry
reactant	2.034, 2.073, 2.025, 2.025, 2.073, 1.981	−/3.736	0	0	0	C_1
A mechanism						
TS	2.090, 2.095, 2.056, 2.044, 2.069, 2.072	2.599/−	20.6	11.1	−3.8	C_1
intermediate	2.109, 2.086, 2.112, 2.153	−/−	18.4	5.0	−5.7	$\sim C_2$
D mechanism						
TS_I	1.988, 2.042, 1.950, 2.071, 1.933	2.813/3.750	16.9	21.9	+0.7	C_1
$intermediate_I$	1.915, 2.052,1.968	−/3.711	1.8	13.1	+0.7	$\sim C_2$
TS_{II}	1.987, 2.125, 2.045, 1.896	2.753/3.765	19.7	25.0	+0.8	$\sim C_s$
$intermediate_{II}$	1.965, 2.046, 1.883	−/3.677	3.9	13.2	+1.2	$\sim C_{2v}$
TS_{III}	1.965, 2.086, 1.951, 2.023, 1.943	2.901/3.695	16.7	22.0	+2.3	C_1
TS_{IV}	1.957, 2.064, 1.952, 2.056, 1.938	2.949/3.755	16.0	23.0	+2.0	C_1

[a] Distances are given in Å; relative energies, in kcal/mol; and volume changes, in cm^3/mol. O_I corresponds to the oxygen of a water molecule in the first sphere; $O^{\ddagger}$ refers to the oxygen of an activated ligand; and O_{II} corresponds to the oxygen of a ligand in the second sphere.

a rather short-lived (experimentally undetectable) species, which therefore suggests that an I_d mechanism cannot be ruled out by purely energetic considerations.

Incorporating solvent effect induces several significant modifications. The most important one is that the D pathway becomes the less preferred mechanism. It appears, indeed, that adding the hydration energy correction increases the activation barrier for the D pathway by about 5.6 kcal/mol while at the same time the $\Delta E^{\ddagger}$ values for the concerted reaction paths are almost unaffected (see Table 2). As a side effect, the lifetime of the D intermediate is increased because the energy difference from the transition state is now equal to 3.0 kcal/mol. However, it still might be difficult to be observed experimentally ($\tau = 3$ ns).

These results are consistent with the expected effects resulting from the calculation of ΔG_{solv}, as previously discussed by Vallet et al.[13] In such charged systems, the electrostatic terms give the major contribution to the hydration energy. As the electrostatic interactions decrease with the increasing size of the cavity, one would therefore expect that, for reaction paths in which the transition state is significantly less compact (positive $\Delta V^{\ddagger}$ value) as compared to the reactant, an increase in the activation barrier would occur. This is precisely the case for the D mechanism for which we calculated a $\Delta V^{\ddagger}_{PCM}$ value of +6.9 cm^3/mol. For the two concerted pathways, the $\Delta V^{\ddagger}_{PCM}$ values are calculated to be almost zero, leading therefore to only small modifications of the activation barriers when taking into account the solvation energy.

A closer examination of the geometries of the two transition states of the interchange mechanism shows that the distances between the metal and the activated water molecules are quite different (see Table 2). We observe indeed that for TS_{trans} those values are 0.10 Å shorter than the ones for TS_{cis}, leading for the latter to a tiny positive $\Delta V^{\ddagger}_{PCM}$ value whereas for the former we have a small negative value for the activation volume. On this basis and taking into account all of the $\Delta E^{\ddagger}_{PCM}$ values, the water-exchange mechanism of $[V(H_2O)_6]^{2+}$ would be deduced to follow an almost purely concerted mechanism (TS_{cis}), with a residual difference between the computed activation barrier in solution and the experimental $\Delta H^{\ddagger}$ value of 2.6 kcal/mol, at the B3LYP level of theory. However, it should be pointed out that the $\Delta V^{\ddagger}_{PCM}$ quantities should be taken with caution. It may happen, indeed, that changing some parameters in the theoretical model may affect those values in one way or another. This is one of the reasons that (see Computational Details) we have also investigated most of the water-exchange pathways with the recently introduced PBE1PBE functional.[43,44] In that case, the $d(V-O)$ distances for the activated water molecules are reduced to 2.721 Å (TS_{cis}) and 2.687 Å (TS_{trans}), and the computed $\Delta V^{\ddagger}_{PCM}$ values are now −1.4 cm^3/mol and −0.8 cm^3/mol, respectively. For the $\Delta E^{\ddagger}$ values, we obtained 17.6 kcal/mol (TS_{cis}) and 20.9 kcal/mol (TS_{trans}) in vacuo, and we found 15.8 and 19.5 kcal/mol in solution. These results would therefore rather predict the water-exchange mechanism to be of the I_a type, the D activation barrier being larger in solution (21.1 kcal/mol), as with the B3LYP functional.

We have shown in this section that density functional theory leads to different activation energies between the dissociative and interchange mechanisms at the gas-phase level, the preference being for the D mechanism. However, when taking into account the effect of the bulk solvent with a polarizable continuum model, one of the interchange pathways becomes preferred because of unfavorable changes in the electrostatic contributions to the hydration energy for the dissociative reaction path; those modifications were related to the variation of the cavity volume during the process. The final result is in agreement with both the experimental data and the theoretical investigation of Rotzinger[9] concerning the concerted nature of the water-exchange mechanism. We should expect, in the case of the water exchange in $[V(H_2O)_6]^{3+}$, that the perturbations induced by the hydration-energy correction would be even larger because we will have to consider here a trivalent metal ion.

Water Exchange in Hydrated V(III). For $[V(H_2O)_6]^{3+}$, the experimental activation volume and activation enthalpy were calculated to be −8.9 cm^3/mol [45] and 11.7 kcal/mol, respectively. From the significant dependence of $\Delta V^{\ddagger}$ on pressure, it was concluded that the I_a mechanism was preferred.[46]

As for V(II), the results of the quantum chemical studies carried out on $[V(H_2O)_6]^{3+}$ are somewhat contradictory. On one hand, Åkesson et al.[2] predicted an interchange mechanism in agreement with experimental data. On the other hand, Rotzinger[4] localized a transition state for which the imaginary mode described the entering/leaving motion of only one water molecule and calculated a relatively long-lived heptacoordinated intermediate ($\tau = 1.3$ ns; $\Delta E_{TS-intermediate} = 2.9$ kcal/mol) of C_2 symmetry. For the D pathway, the pentacoordinated intermediate was shown to lie above the other transition state, thus precluding the requirement of a full investigation for this particular reaction path. From these results, the activation process was identified as an A mechanism.

Table 3 summarizes the results of our DFT investigation of the water-exchange mechanisms of $[V(H_2O)_6]^{3+}$. From the five transitions states that have been computed, four of them (TS_I, TS_{II}, TS_{III}, TS_{IV}) correspond to a D mechanism, as indicated by their imaginary mode that describes the motion of only one activated ligand, their positive activation volume, and when

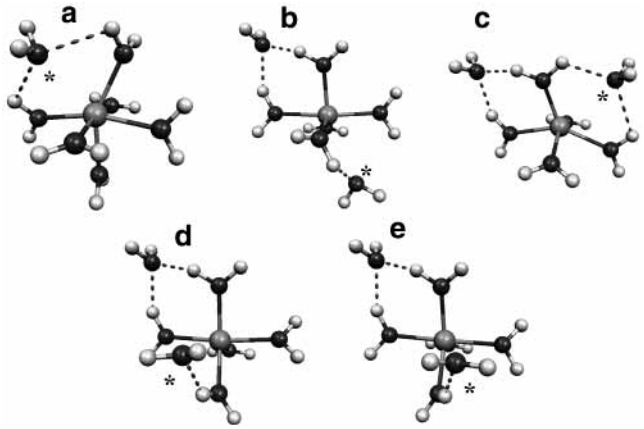

Figure 4. Optimized geometries of the transition states for the water-activation processes of $[V(H_2O)_6]^{3+}$. (a) A mechanism, (b) D mechanism: TS_I, (c) D mechanism: TS_{II}, (d) D mechanism: TS_{III}, and (e) D mechanism: TS_{IV}. The activated water molecules are marked with a star .

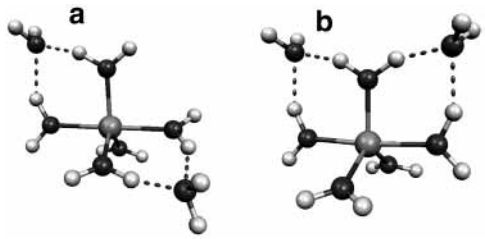

Figure 5. Optimized structures of the intermediates of D pathways on $[V(H_2O)_6]^{3+}$. (a) intermediate$_I$ and (b) intermediate$_{II}$.

available, the presence of a pentacoordinated intermediate. Among them, TS_{III} and TS_{IV} will be considered together because they show significant geometrical similarities (see Figure 4d and e). Moreover, the calculation of the intrinsic reaction coordinate toward an intermediate led, in both cases, to the deprotonation of a water ligand of the first sphere by the leaving H_2O molecule. This feature is reminiscent of the behavior we observed when we tried to optimize the reactant with the seventh water molecule in the terminal position. As previously discussed, this is clearly an artifact that can be attributed to the omission of explicit additional coordination spheres. For the two others dissociative reaction profiles, the transition states could be connected to stable intermediates (see Figure 5). Those minima exhibit a similar trigonal bipyramidal pentacoordinated structure with the water molecules in the second coordination sphere that are hydrogen bonded to two ligands of the first hydration shell. In one case, the corresponding water molecules are cis to each other, and in the other case, they are in the trans position. Similar complexes have already been computed as stable structures by other investigators for Zn(II)[5] and Ga(III),[6] but the localization of the transition states that connect those minima to the reactant was either not successful or was not attempted. However, Hartmann et al.[7] obtained a structure related to one of ours (intermediate$_I$) when they carried out a density functional investigation of the water-exchange mechanism of $[Ti(H_2O)_5(OH)]^{2+}\cdot H_2O$. Finally, for the fifth reaction path, we calculated a negative $\Delta V^{\ddagger}_{PCM}$ value and localized a transition state of C_1 symmetry that could be connected to a heptacoordinated intermediate. Such results allow us to consider that this transition state is indicative of an associative pathway.

Considering the different gas-phase activation barriers, it appears that contrary to what was obtained by Rotzinger [4] using ab initio methods the D pathways cannot be excluded at the B3LYP level of theory because they are in fact the preferred ones. TS_I-TS_{IV} are indeed found to lie between 0.9 kcal/mol (TS_{II}) and are up to more than 3.7 kcal/mol (TS_I-TS_{III-IV}) lower in energy than the associative transition state. The fact that TS_{II} is computed to be the least stable of the D transition-state structures seem to be consistent with its hindered conformation. The activated ligand is indeed located in the symmetry plane of the complex at the shortest $V-O^{\ddagger}$ distance of all of these transition states (see Table 3 and Figure 4c).

To conclude the analysis of the gas-phase reaction paths, it should be noted that the stability of the heptacoordinated and available pentacoordinated species is completely different. For the associative reaction, the energy difference between the transition state and the intermediate is small ($\Delta E_{TS-intermediate} = 2.2$ kcal/mol). On the contrary, the pentacoordinated species are deeply stabilized and computed to lie only 1.8 kcal/mol (TS_I) and 3.9 kcal/mol (TS_{II}) above the reactant. These latter results are somewhat surprising, but it should be noted that in their investigation of the D mechanism on $[Ti(H_2O)_5(OH)]^{2+}$ Hartmann et al. [7] obtained a trans intermediate that was almost as stable as the reactant. As we will see in the next section, taking into account solvent effects will, among other things, moderate these findings.

As for hexaaquavanadium(II), a changeover of the preferred exchange mechanism occurs on going from the gas phase to the solution. The $\Delta E^{\ddagger}_{PCM}$ values of all dissociative reaction pathways are now significantly larger (by more than 10 kcal/mol) than the corresponding value for the A mechanism. More precisely, adding the hydration energy leads for the A pathway to a net decrease of 9.5 kcal/mol of its activation barrier while at the same time a smaller increase of the D activation energies can be noted. Here again, the observed evolution of the $\Delta E^{\ddagger}$ values in solution can be linked to variations of the cavity volumes and hence to modifications of the electrostatic terms in ΔG_{solv} between the reactant and the different transition states. For the associative mechanism, we have a transition state that is more compact than the reactant ($\Delta V^{\ddagger} < 0$); therefore, the electrostatic contributions to the solvation energy are larger for the former (−417.7 kcal/mol) than for the latter (−409.3 kcal/mol). For the different transition states of the D mechanisms, the electrostatic terms are found to be smaller, ranging from −403.1 kcal/mol (TS_{III}) to −404.8 kcal/mol (TS_{II}), because of the increase of the cavity size of the complex on going from the reactant to the transition states.

Taking into account the hydration energy also induces strong perturbations of the intermediates' stability. The depth of the potential energy surface well for the A intermediate has been increased by nearly 4 kcal/mol, leading therefore in solution to a species of longer lifetime. Meanwhile, the two pentacoordinated structures have been destabilized as compared to the reactant by about 10 kcal/mol. Because the activation barriers were raised only by about 5 kcal/mol, it appears that they are now located 8.8 kcal/mol (TS_I) and 11.8 kcal/mol (TS_{II}) below their respective transition states. Taken as a whole, the various perturbations induced by the solvent lead therefore to a better description of the water-exchange mechanism. As a final statement, we point out that contrary to $[V(H_2O)_6]^{2+}$ we obtain here a much better agreement of the computed activation energy with the $\Delta H^{\ddagger}$ value because the difference in solution is equal to 0.6 kcal/mol.

Conclusions

In the present work, density functional calculations have been carried out on hexahydrated vanadium cations both in vacuo and in aqueous solution. It has been shown that the solvent

effects are of paramount importance in achieving a satisfactory description of both the structure and the water-exchange mechanisms of $[V(H_2O)_6]^{2+/3+}$. We showed that taking into account an explicit second coordination sphere leads to significant distortions of the $[V(H_2O)_6]^{3+}$ complex, which was found to be of C_i symmetry in the gas phase. From the two conformers presented in this paper, the most stable one exhibits a wheel-like structure of near-S_6 symmetry in which $[V(H_2O)_6]^{3+}$ was found to recover an almost perfect D_{3d} symmetry. This arrangement was characterized in the neutron diffraction experiment on $[V(H_2O)_6][H_5O_2](CF_3SO_3)_4$.[31] The other form, of D_2 symmetry, was found to be located 15.6 kcal/mol higher in energy at the gas-phase level. This energy difference was found to be even larger when the effect of the bulk solvent was taken into account using a polarizable continuum model. Similar conclusions could be deduced concerning the structure of the preferred conformer and the effect of solvation on $[V(H_2O)_6]^{2+}\cdot(H_2O)_{12}$. Moreover, the study on the conformers of $[V(H_2O)_6]^{3+}\cdot(H_2O)_{12}$ allowed us to demonstrate that the spontaneous deprotonation processes that occurred in some structures of the water-exchange investigation of $[V(H_2O)_6]^{3+}$ were undoubtedly artifacts related to the neglect of solvent effects during the geometry optimizations.

For the water-exchange processes, the DFT calculations in vacuo showed that in all cases the D mechanisms are preferred. Considering the hydration energy, estimated within the PCM method, led to inversions in the water-exchange mechanisms. Consequently, we found the water-exchange mechanism of $[V(H_2O)_6]^{2+}$ to proceed through an I pathway whereas for hexaaquavanadium(III) we found that a limiting A mechanism was in operation at the B3LYP level of theory. The respective activation barriers were computed to be 2.6 kcal/mol higher and 0.6 kcal/mol lower than the experimental $\Delta H^{\ddagger}$ values. All of the above results emphasize the importance of the solvent effects, and they show that the calculation of the solvation energy cannot be avoided for the investigation of such charged species using density functional theory.

References and Notes

(1) Ritchens, D. T. *The Chemistry of Aqua Ions: Synthesis, Structure, and Reactivity: A Tour Through the Periodic Table of the Elements*; Wiley: Chichester, U.K., 1997.

(2) Åkesson, R.; Pettersson, L. M. G.; Sandström, M.; Wahlgren, U. *J. Am. Chem. Soc.*, **1994**, *116*, 8705.

(3) Rotzinger, F. P. *J. Am. Chem. Soc.* **1996**, *118*, 6760.

(4) Rotzinger, F. P. *J. Am. Chem. Soc.* **1997**, *119*, 5230.

(5) Hartmann, M.; Clark, T.; van Eldik, R. *J. Am. Chem. Soc.* **1997**, *119*, 7843.

(6) Kowall, Th.; Caravan, P.; Bourgeois, H.; Helm, L.; Rotzinger, F. P.; Merbach, A. E. *J. Am. Chem. Soc.* **1998**, *120*, 6569.

(7) Hartmann, M.; Clark, T.; van Eldik, R. *J. Phys. Chem. A* **1999**, *103*, 9899.

(8) Rotzinger, F. P. *J. Phys. Chem. A* **1999**, *103*, 9345.

(9) Rotzinger, F. P. *Helv. Chim. Acta* **2000**, *83*, 3006.

(10) Rotzinger, F. P. *J. Phys. Chem. A* **2000**, *104*, 6439.

(11) Rotzinger, F. P. *J. Phys. Chem. A* **2000**, *104*, 8787.

(12) De Vito, D.; Sidorenkova, H.; Rotzinger, F. P.; Weber, J.; Merbach, A. E. *Inorg. Chem.* **2000**, *39*, 5547.

(13) Vallet, V.; Wahlgren, U.; Schimmelpfennig, B.; Moll, H.; Szabó, Z.; Grenthe, I. *J. Am.. Chem. Soc.* **2001**, *123*, 11999.

(14) Inada, Y.; Mohammed, A. H.; Loeffler, H. H.; Rode, B. M. *J. Phys. Chem. A* **2002**, *106*, 6783.

(15) Onsager, L. *J. Am. Chem. Soc.* **1936**, *58*, 1486.

(16) Miertus, S.; Scrocco, E.; Tomasi, J. *Chem. Phys.* **1981**, *55*, 117.

(17) Miertus, S. E.; Tomasi, J. *Chem. Phys.* **1982**, *65*, 239.

(18) Cossi, M.; Barone, V.; Cammi, R.; Tomasi, J. *Chem. Phys. Lett.* **1996**, *255*, 327.

(19) Frisch, M. J.; Trucks, G. W.; Schlegel, H. B.; Scuseria, G. E.; Robb, M. A.; Cheeseman, J. R.; Zakrzewski, V. G.; Montgomery, J. A., Jr.; Stratmann, R. E.; Burant, J. C.; Dapprich, S.; Millam, J. M.; Daniels, A. D.; Kudin, K. N.; Strain, M. C.; Farkas, O.; Tomasi, J.; Barone, V.; Cossi, M.; Cammi, R.; Mennucci, B.; Pomelli, C.; Adamo, C.; Clifford, S.; Ochterski, J.; Petersson, G. A.; Ayala, P. Y.; Cui, Q.; Morokuma, K.; Malick, D. K.; Rabuck, A. D.; Raghavachari, K.; Foresman, J. B.; Cioslowski, J.; Ortiz, J. V.; Stefanov, B. B.; Liu, G.; Liashenko, A.; Piskorz, P.; Komaromi, I.; Gomperts, R.; Martin, R. L.; Fox, D. J.; Keith, T.; Al-Laham, M. A.; Peng, C. Y.; Nanayakkara, A.; Gonzalez, C.; Challacombe, M.; Gill, P. M. W.; Johnson, B. G.; Chen, W.; Wong, M. W.; Andres, J. L.; Head-Gordon, M.; Replogle, E. S.; Pople, J. A. *Gaussian 98*, revision A.11.3; Gaussian, Inc.: Pittsburgh, PA, 1998.

(20) Becke, A. D. *J. Chem. Phys.* **1993**, *37*, 5648.

(21) Lee, C.; Yang, R. G.; Parr, R. G. *Phys. Rev. B* **1988**, *37*, 785.

(22) McLean, A. D.; Chandler, G. S. *J. Chem. Phys.* **1980**, *72*, 5639.

(23) Krishnan, R.; Binkley, J. S.; Seeger, R.; Pople, J. A. *J. Chem. Phys.* **1980**, *72*, 650.

(24) Wachters, A. J. H. *J. Chem. Phys.* **1970**, *52*, 1033.

(25) Hay, P. J. *J. Chem. Phys.* **1977**, *66*, 4377.

(26) Ditchfield, R.; Hehre, W. J.; Pople, J. A. *J. Chem. Phys.* **1971**, *54*, 724.

(27) Hehre, W. J.; Ditchfield, R.; Pople, J. A. *J. Chem. Phys.* **1972**, *56*, 2257.

(28) Holt, D. G.; Larkworthy, L. F.; Povey, D. C.; Leigh, G. J. *Inorg. Chim. Acta* **1990**, *169*, 201.

(29) Cotton, F. A.; Daniels, L. M.; Murillo, C. A.; Quesada, J. F. *Inorg. Chem.* **1993**, *32*, 4861.

(30) Best, J. K.; Best, S. P. *Coord. Chem. Rev.* **1997**, *166*, 391 and references therein.

(31) Cotton, F. A.; Fair, C. K.; Lewis, G. E.; Mott, G. N.; Ross, F. K.; Schultz, A. J.; Williams, J. M. *J. Am. Chem. Soc.* **1984**, *106*, 5319.

(32) Kallies, B.; Meier, R. *Inorg. Chem.* **2001**, *40*, 3101.

(33) Reed, A.; Curtiss, L. A.; Weinhold, F. *Chem. Rev.* **1988**, *88*, 899.

(34) Xantheas, S. S. *J. Chem. Phys.* **1995**, *102*, 4505.

(35) Uudsemaa, M.; Tamm, T. *Chem. Phys. Lett.* **2001**, *342*, 667.

(36) Markham, G. D.; Glusker, J. P.; Bock, C. W. *J. Phys. Chem. B* **2002**, *106*, 5118.

(37) Pye, C. C.; Rudolph, W. W. *J. Phys. Chem. A* **1998**, *102*, 9933.

(38) Rotzinger, F. P. *J. Chem. Soc., Dalton Trans.* **2002**, 719.

(39) Baes, C. K.; Mesmer, R. E. *The Hydrolysis of Cations*; Robert E. Krieger Publishing Company: Malabar, FL, 1986.

(40) Ducommun, Y.; Zbinden, D.; Merbach, A. E. *Helv. Chim. Acta*, **1982**, *65*, 1385.

(41) Swaddle, T. W.; Mak, M. K. S. *Can. J. Chem.* **1983**, *61*, 473.

(42) Vallet, V.; Wahlgren, U.; Schimmelpfennig, B.; Moll, H.; Szabó, Z.; Grenthe, I. *Inorg. Chem.* **2001**, *40*, 3516.

(43) Perdew, J. P.; Burke, K.; Ernzerhof, M. *Phys. Rev. Lett.* **1996**, *77*, 3865.

(44) Perdew, J. P.; Burke, K.; Ernzerhof, M. *Phys. Rev. Lett.* **1997**, *78*, 1396.

(45) Hugi, A. D.; Helm, L.; Merbach, A. E. *Helv. Chim. Acta*, **1985**, *68*, 508.

(46) Helm, L.; Merbach, A. E. *Coord. Chem. Rev.* **1999**, *187*, 151.